

Groundwater quality evaluation and source analysis in typical karst areas

SHI YU

yushihydrogeo@163.com

1 Karst Dynamics Laboratory, Ministry of Land and Resources/Guangxi;

2 Institute of Karst Geology, Chinese Academy of Geological Sciences; 3 International Research Center on Karst Under the Auspices of UNESCO,



Outline

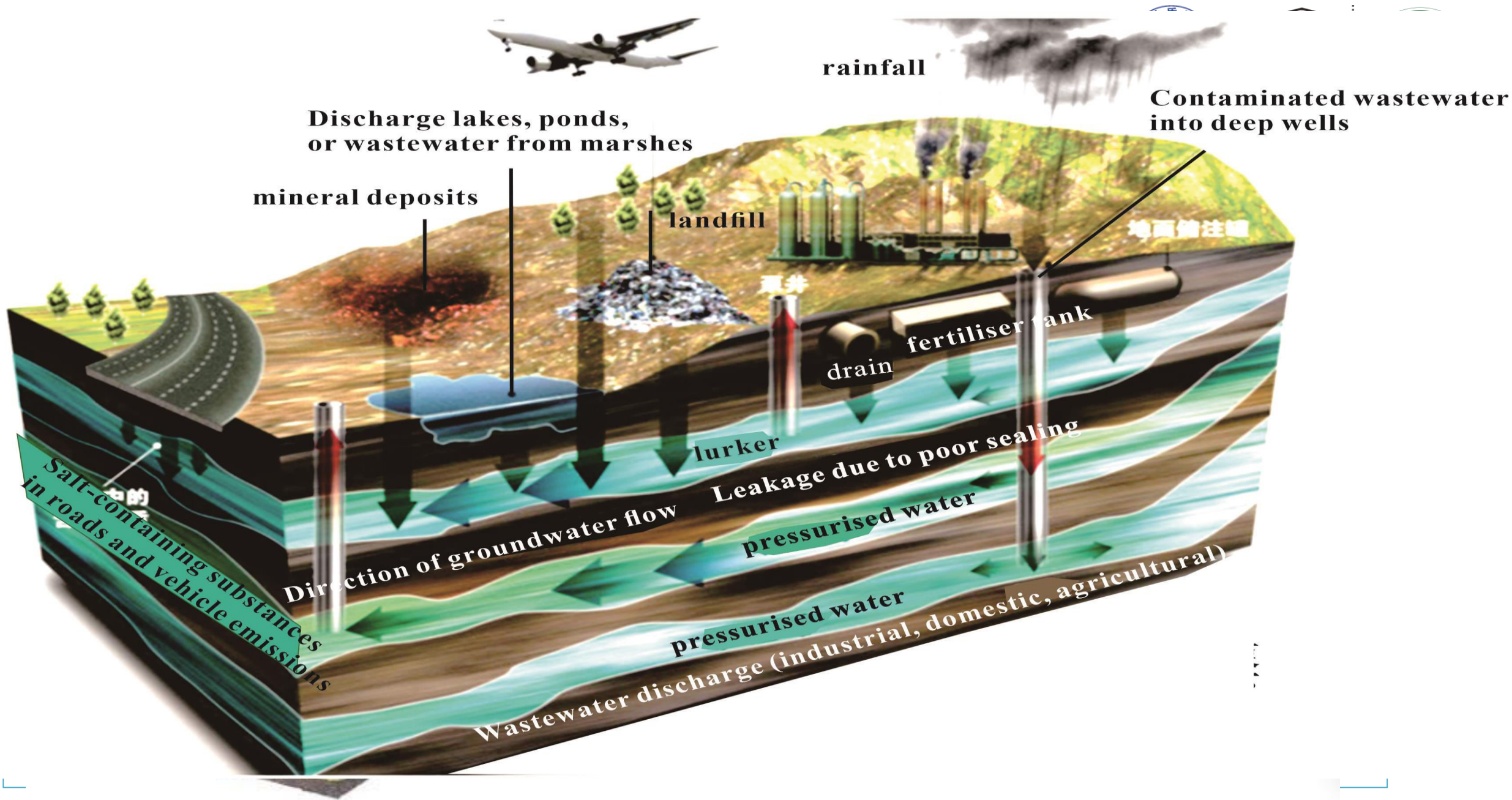
1. Introduction

2. Research highlights

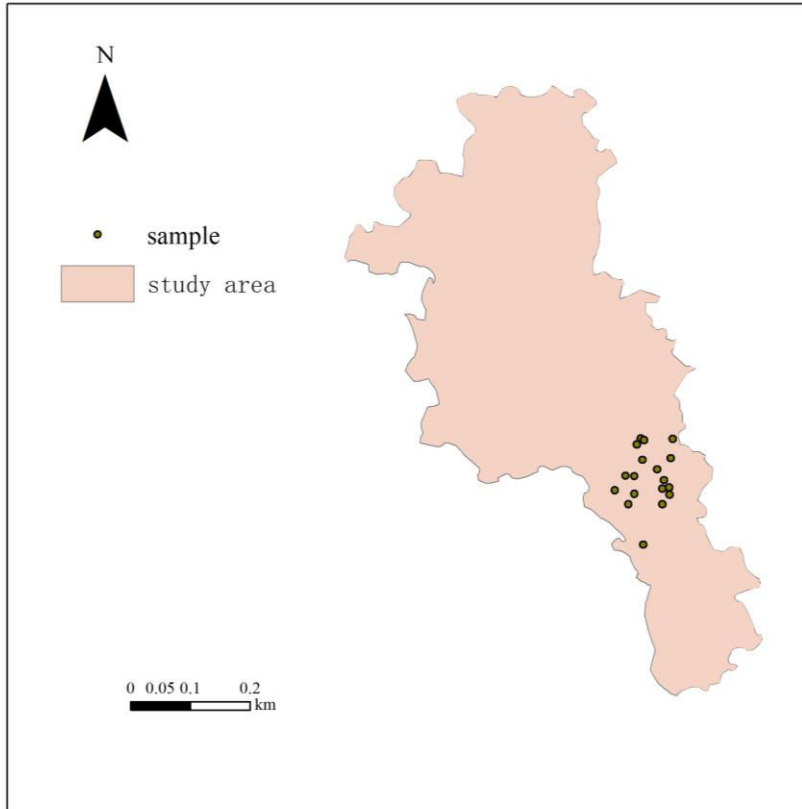
3. Site description and Methods

4. Discussion

5. Summary

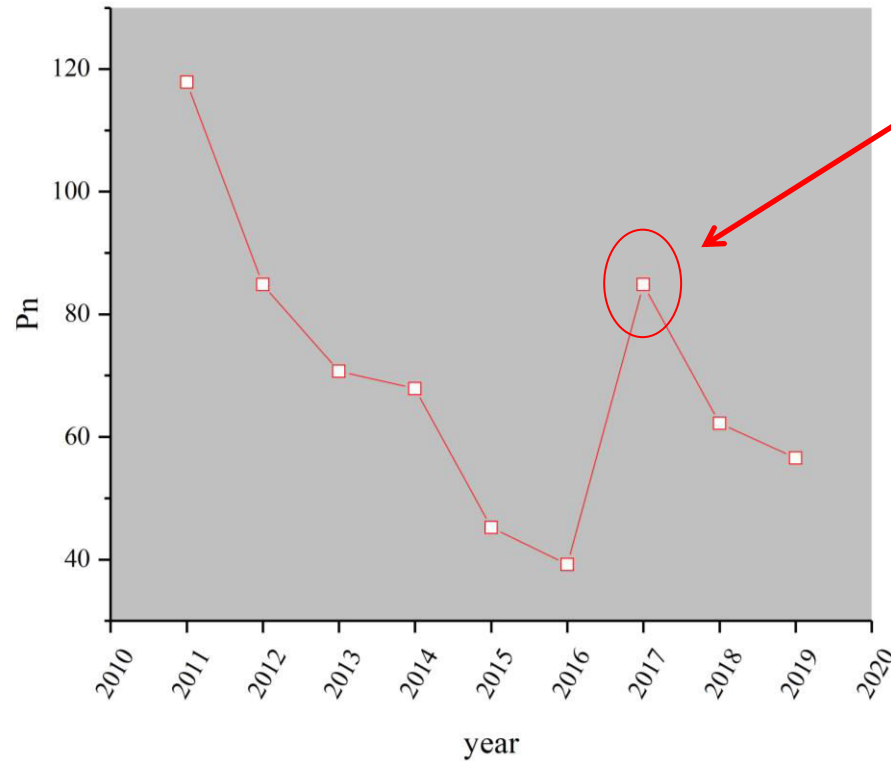


2. Research highlights



Study area map of Lingui District, Guilin

- Important industrial base and transport hub of Guilin City
- Area 2190.27 km²

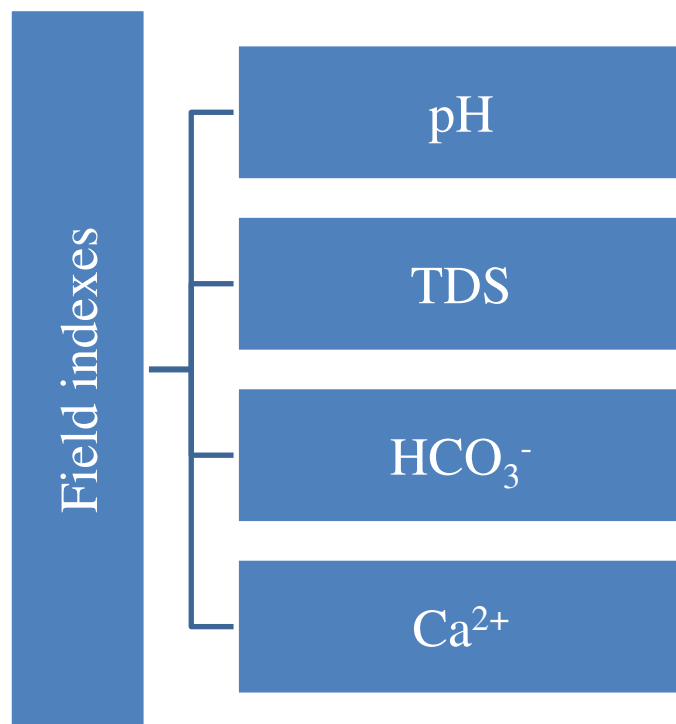


Water quality shifts in 2017

- Therefore, **the specific pollution sources and main pollution factors** of its water quality from 2017 -2019 were selected for analysis.

3. Site Description and Methods

Water chemical parameters



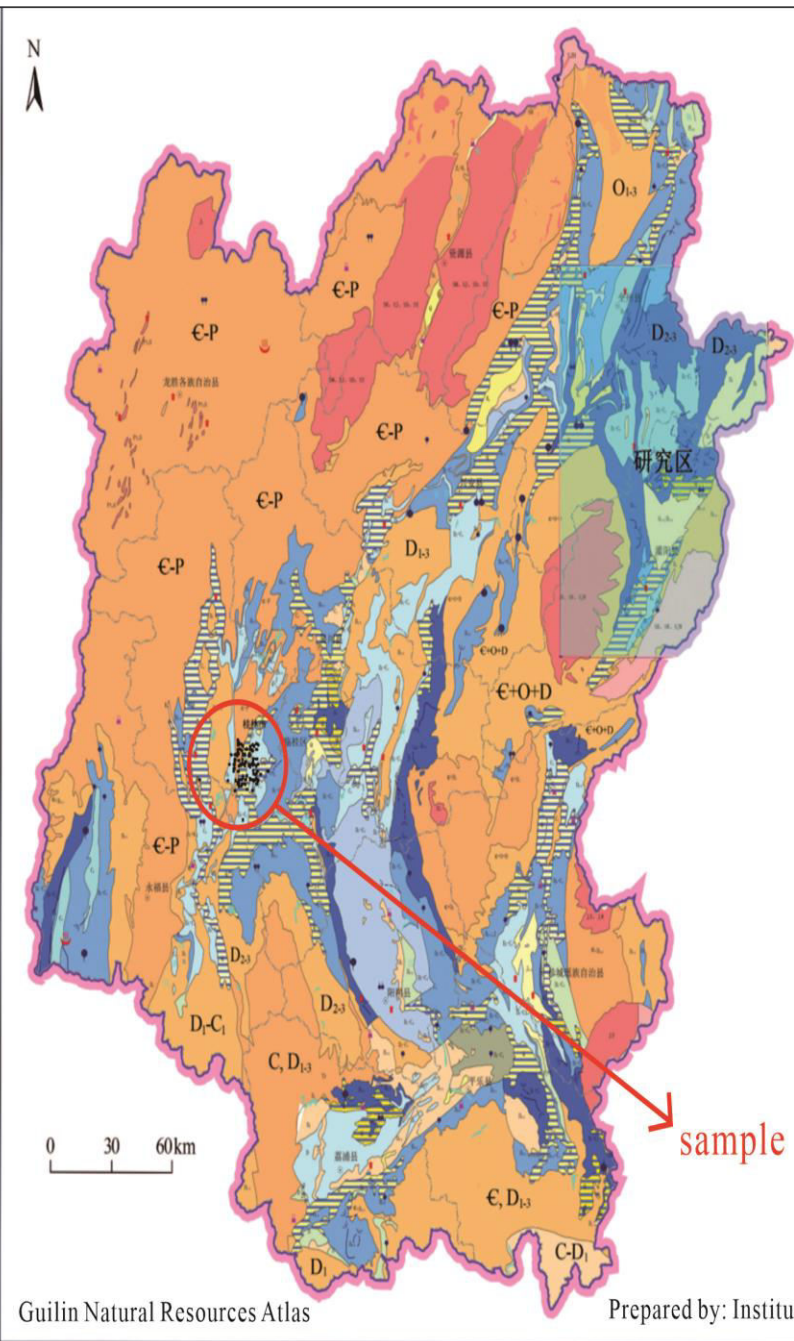
Laboratory analysis

• Main factors

K^+ 、 Na^+ 、 Ca^{2+} 、 Mg^{2+} 、 SO_4^{2-} 、 NO_3^- 、 HCO_3^- 、 Cl^- 、 F^-

Pb、As、Hg、Zn、Mn、Fe





Prepared by: Institute of Karst Geology, China Geological Survey
 Compilation date: October 2018

Groundwater types and water abundance

- Abundant water volume
- Moderate water volume
- Water scarcity

Carbonate karst water

- Abundant water volume
- Moderate water volume
- Water scarcity

Carbonate rock mixed with clastic rock fissure karst cave water

- Abundant water volume
- Moderate water volume
- Water scarcity

Clastic rock mixed with carbonate rock karst cave fissure water

- Moderate water volume
- Water scarcity

covered karst

- Overlying Quaternary pore water
- Below is carbonate karst water

Bedrock fissure water

- Abundant water volume
- Moderate water volume
- Water scarcity

Magmatic rock fissure water

- Abundant water volume
- Moderate water volume
- Water scarcity

Hydrologic station

- Traffic station
- Water level station

Control water points

- Underground river and its inlet and outlet
- Daquan
- Descending and Rising Springs
- Spring groups
- Geothermal hot spring
- Underground River Skylight



• **Location**

Guilin city, SW
 China

• **lithology**

Carbonate rocks

• **area**

2190km²



Period

July, 2017

July, 2018

July, 2019



Calculation



(1) Single-Factor pollution Index (P_i)

$$P_i = \frac{C_i}{B_i}$$

C_i : Measured concentrations of factor i

B_i : factor i corresponding environmental standard values

(2) Nemerow Multi-Factor pollution Index (P_n)

$$P_n = \sqrt{\frac{\max(P_i)^2 + \text{ave}(P_i)^2}{2}}$$

$\max(P_i)$: Maximum value of single-factor pollution index for factors

$\text{ave}(P_i)$: Mean values of single-factor pollution indices for each factor

Calculation



The evaluation criteria for the single-factor pollution index P_i and the multi-factor composite pollution index P_n are shown in Table 1.

Table 1 Evaluation criteria of single factor pollution index P_i and multi-factor comprehensive pollution index P_n

P_i	P_n	pollution assessment
$P_i \leq 1$	$P_n \leq 0.7$	No Pollution
$1 < P_i \leq 2$	$0.7 < P_n \leq 1$	Low pollution
$2 < P_i \leq 3$	$1 < P_n \leq 2$	Moderate polluted
$P_i > 3$	$P_n > 2$	Strong polluted



4. Discussion

4.1 Groundwater quality assessment

4.2 Screening of groundwater quality for major pollutants

4.3 Spatial and temporal distribution of the main pollutants of groundwater quality

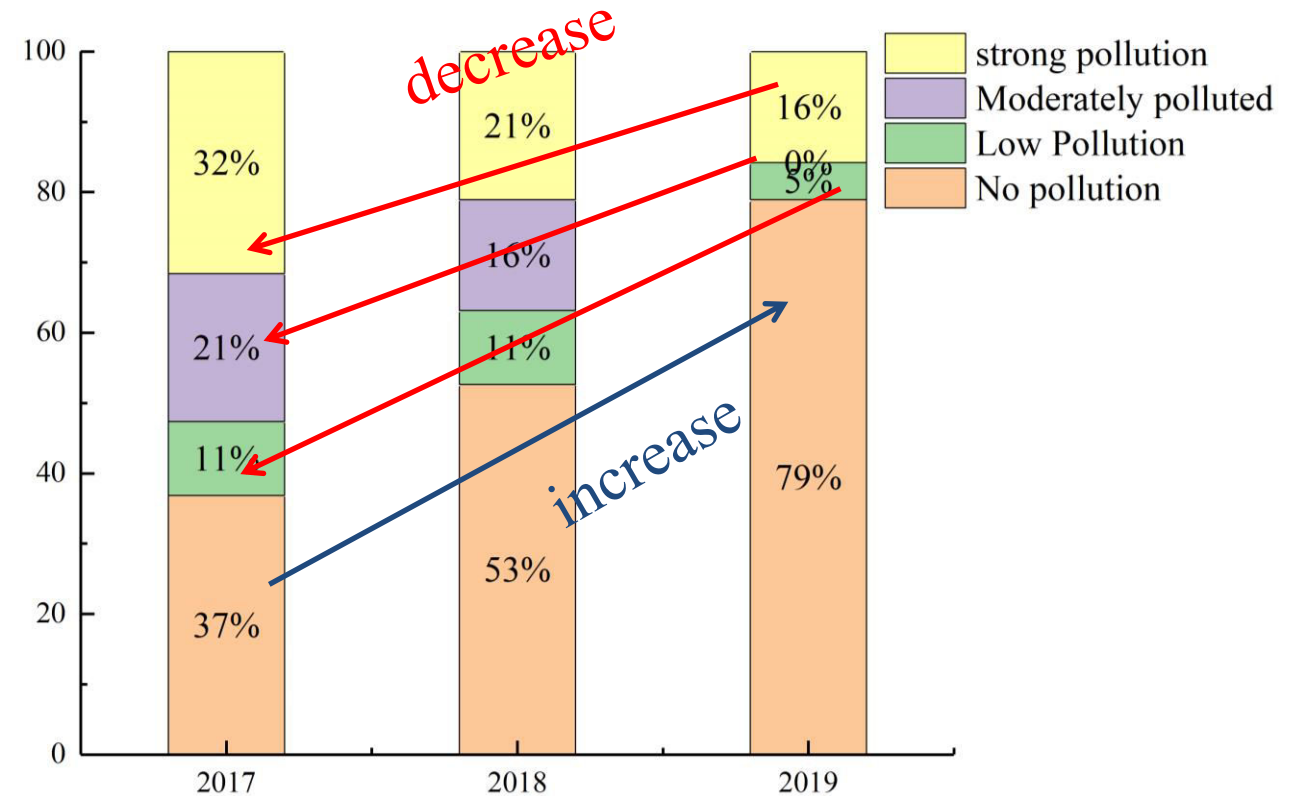
4.4 Source analyses of groundwater quality

4.1 Groundwater quality assessment



Year	Nemerow Multi-Factor pollution Index (P_n)	Degree of contamination
2017	84.85	Strong polluted
2018	62.23	Strong polluted
2019	56.57	Strong polluted

decrease



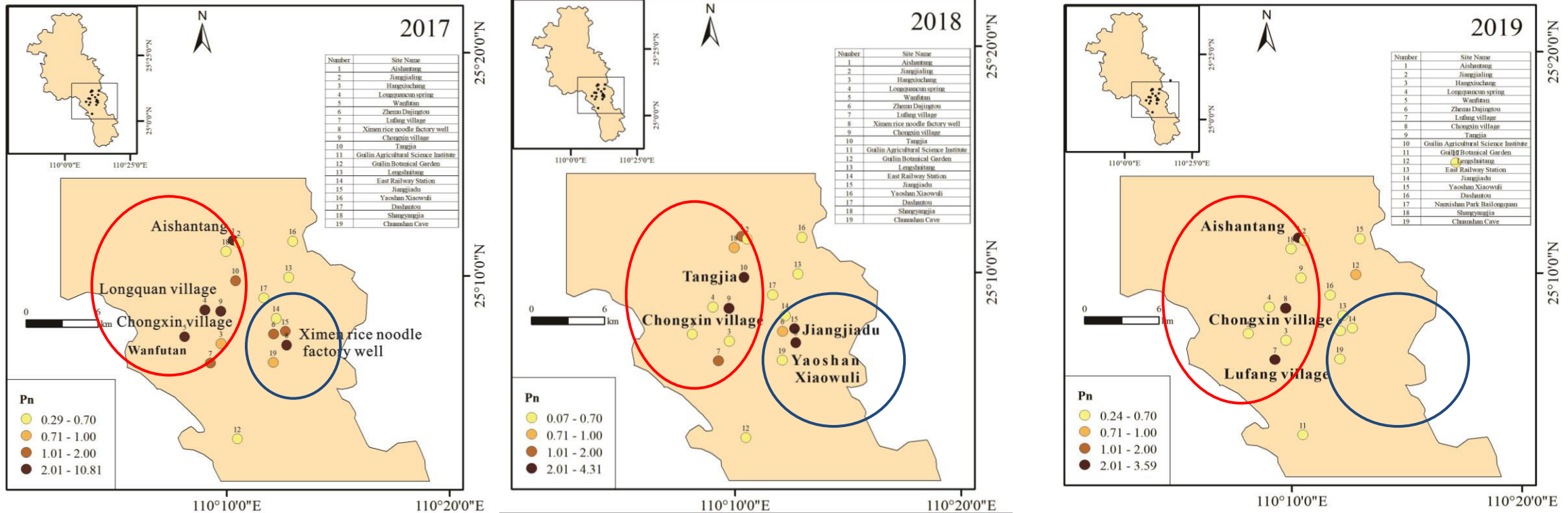
Groundwater Quality Percentage Map for the Study Area

Guilin groundwater quality in terms of time distribution, 2017-2019 with time changes in water quality generally improved. This may be related to the Notice of the General Office of the People's Government of the Guangxi Zhuang Autonomous Region on the “Issuance of Measures for the Management of Groundwater in Guangxi” .

4.1 Groundwater quality assessment

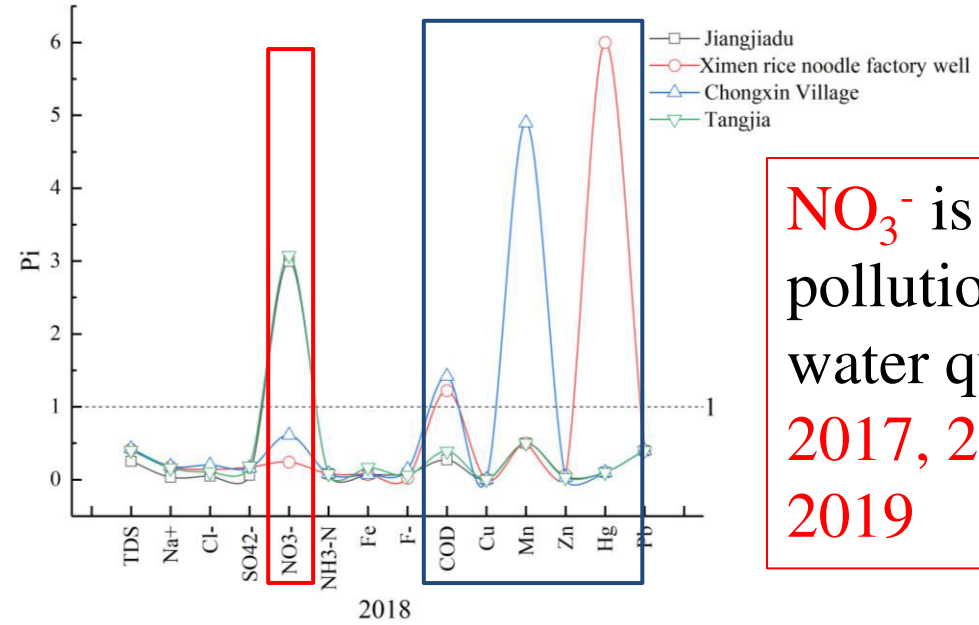
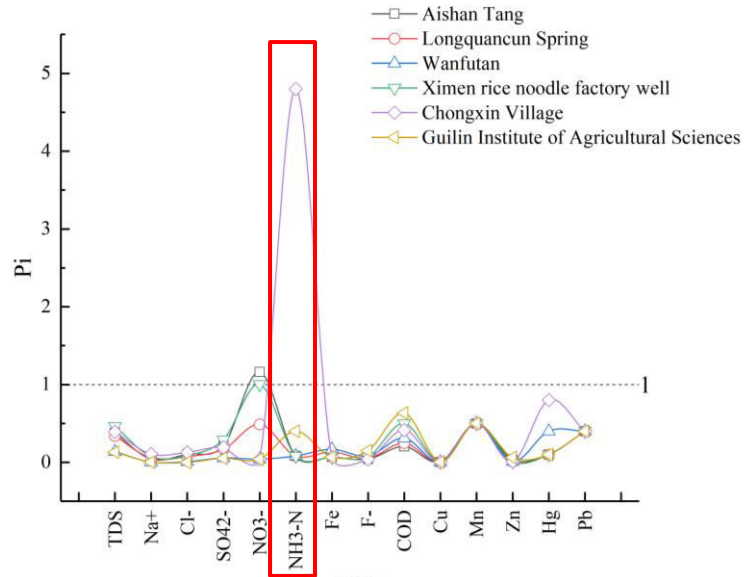


Spatial distribution of pollutant: west is worse than in the east.

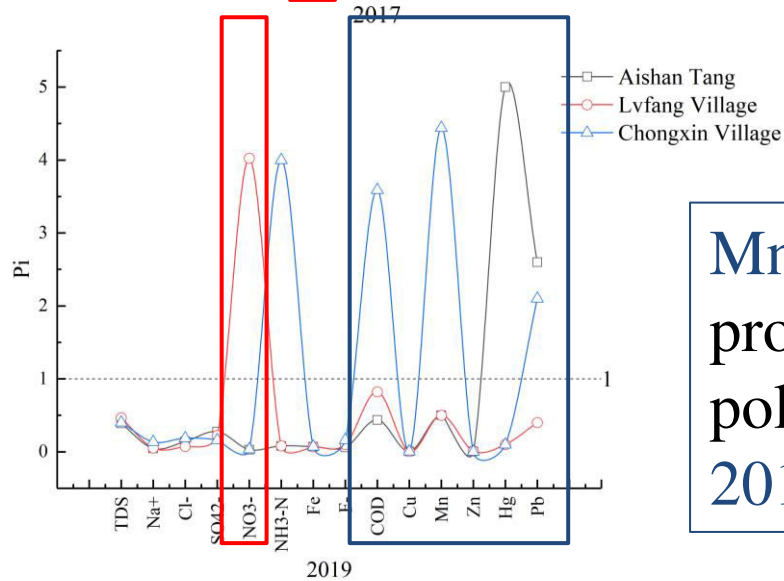


- **Anthropogenic:** due to measures such as centralised disposal of pollutants and enhanced industrial wastewater management since the implementation of the policy in 2017, the water quality of the industrial area in the East District has shown significant improvement.
- **Natural:** the groundwater in the East District has a high degree of karst development, good hydraulic conductivity, strong dilution and self-purification ability, and pollutants are not easy to be enriched in the groundwater (Jia Yannan, 2004), so the water quality is better.

4.2 Screening of groundwater quality for major pollutants



NO₃⁻ is a common pollution factor for water quality in 2017, 2018 and 2019



Mn, Hg, Pb more prominent factors of pollution in 2018 and 2019

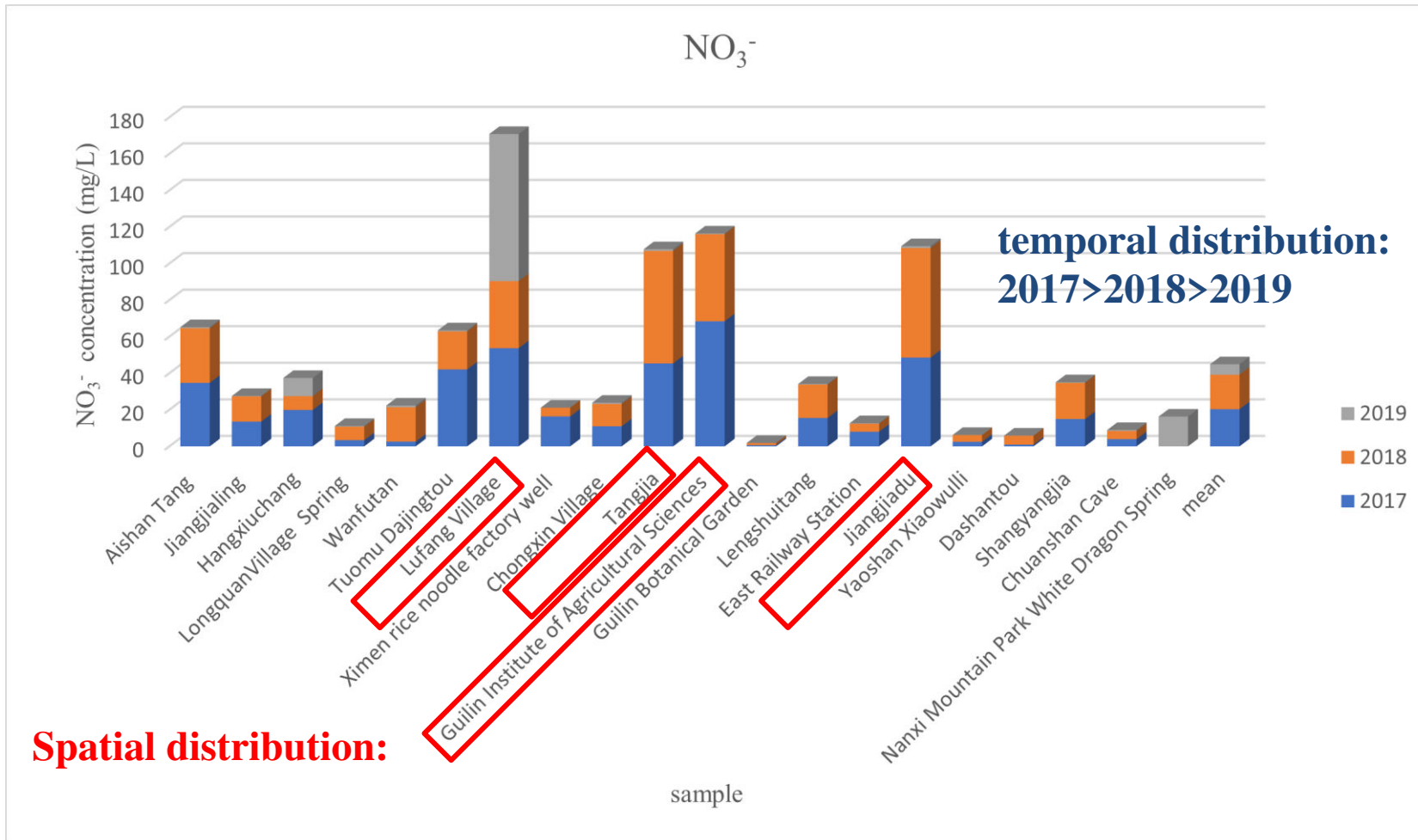
The trend in the evolution of water quality from 2017-2019 is a gradual decrease in pollution, but an increase in the diversity of pollutants.

4.3 Spatial and temporal distribution of the main pollutants of groundwater quality



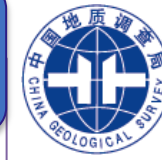
The spatial and temporal distributions of NO_3^- , Mn, Pb, which were screened as the more polluting factors, were analysed in order to analyse the specific causes of pollution.

● **Spatial and temporal distribution of NO_3^-**

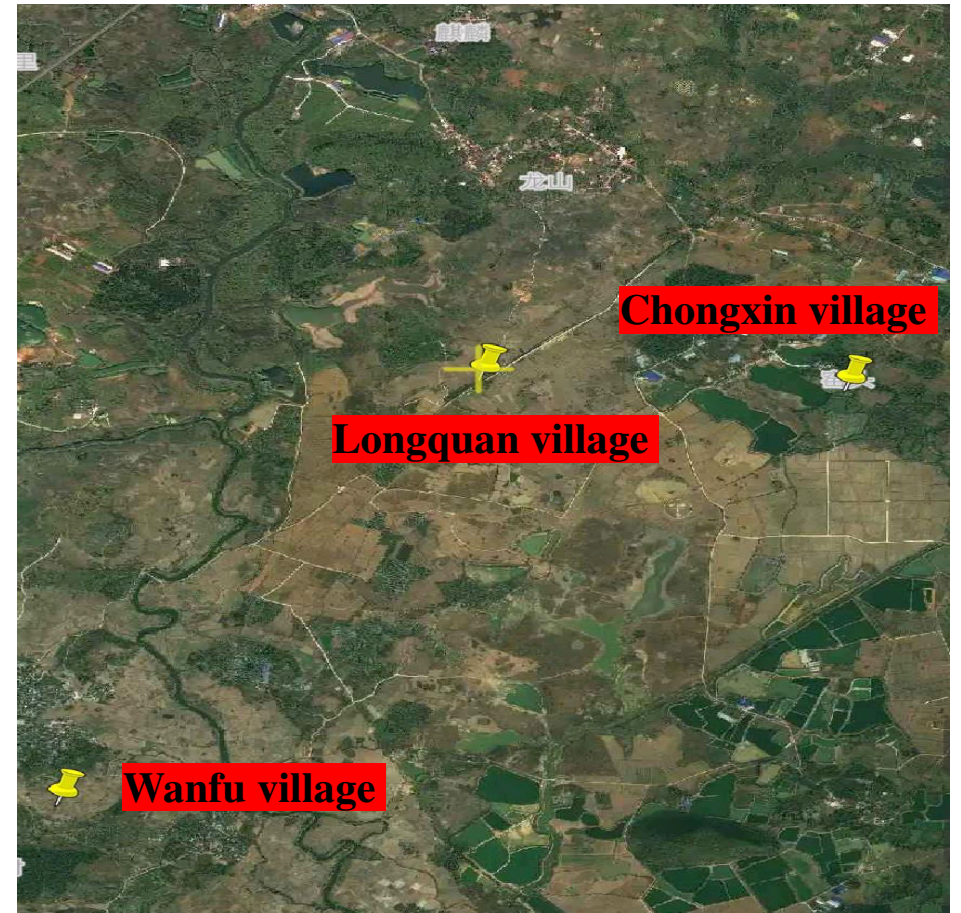
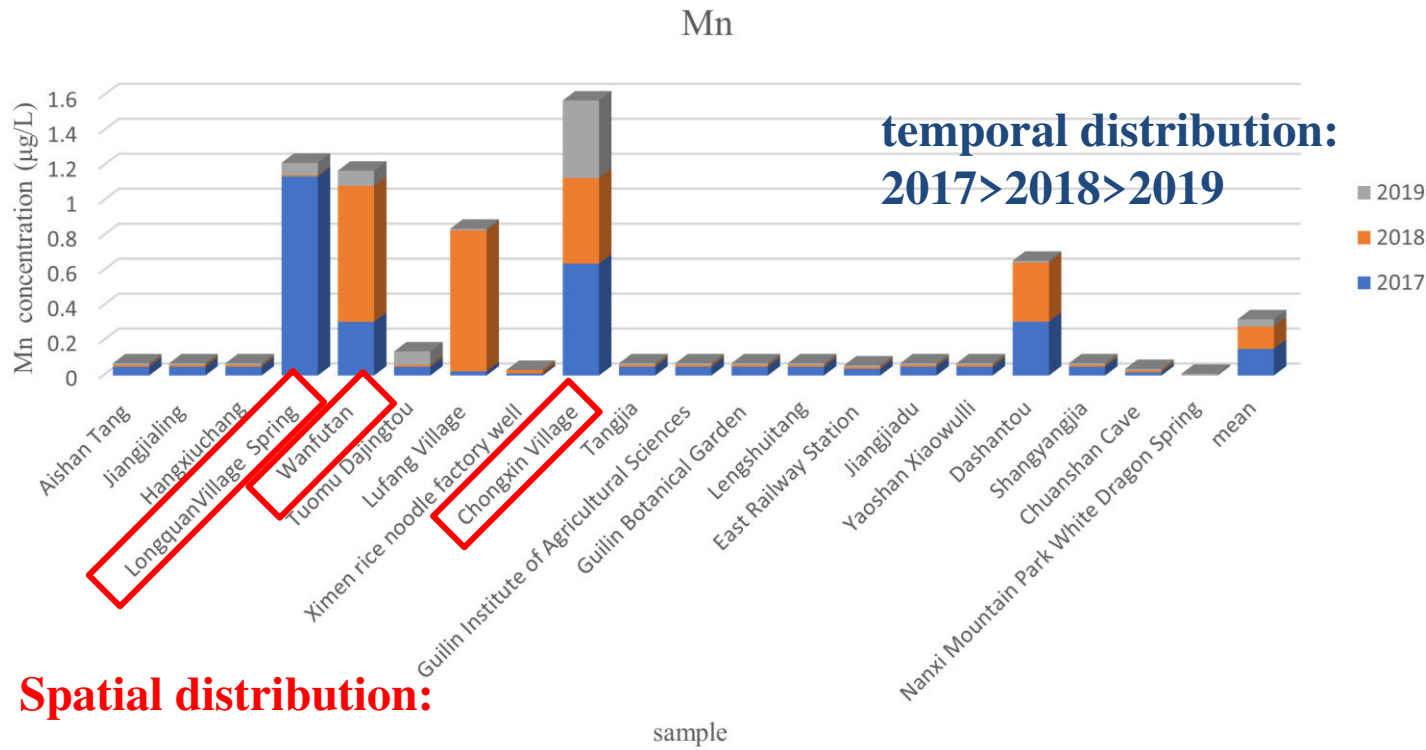


Higher spatial NO_3^- concentrations in **agricultural and residential areas** may be related to the use of agricultural nitrogen **fertilisers** and the infiltration of **domestic sewage**.

4.3 Spatial and temporal distribution of the main pollutants of groundwater quality



● Spatial and temporal distribution of Mn

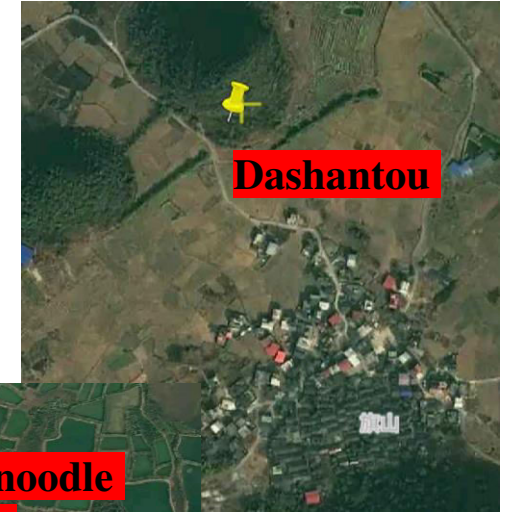
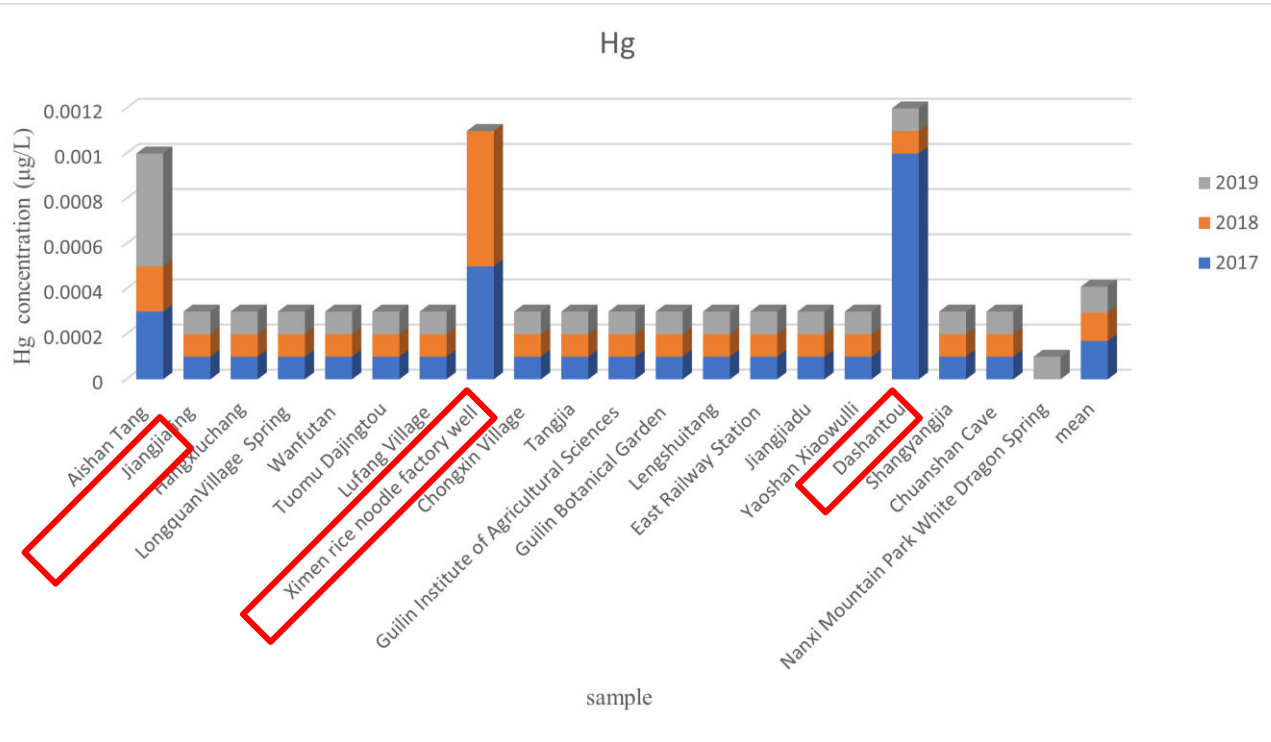


The sampling sites with **high concentrations Mn** were all near water systems and may have been caused by the **discharge of effluents** that allowed manganese to enter the groundwater system.

4.3 Spatial and temporal distribution of the main pollutants of groundwater quality

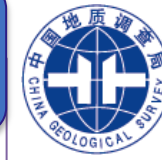


● Spatial and temporal distribution of Hg

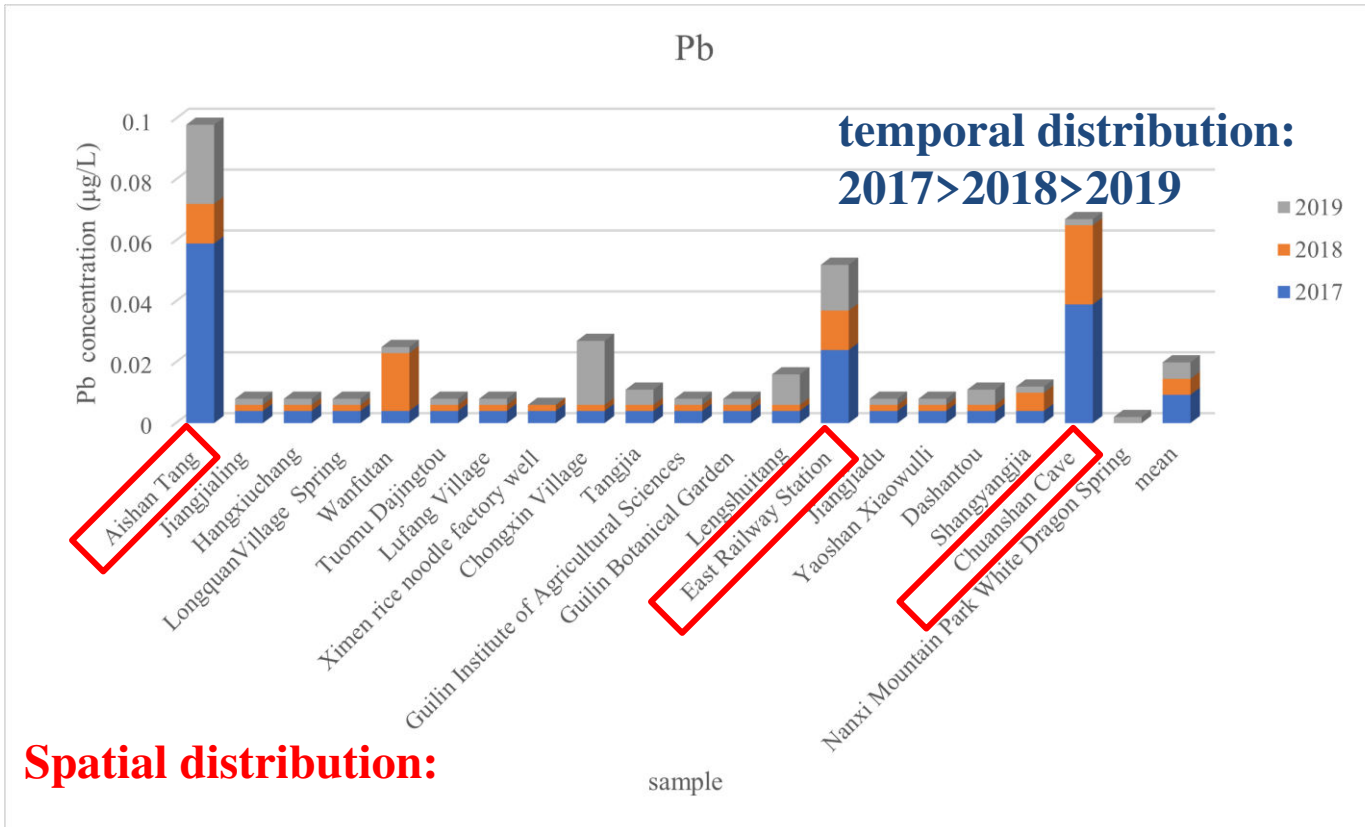


The spatial distribution of Hg is dominated in agricultural land near villages and factories. The temporal distribution of Hg is more evenly distributed.

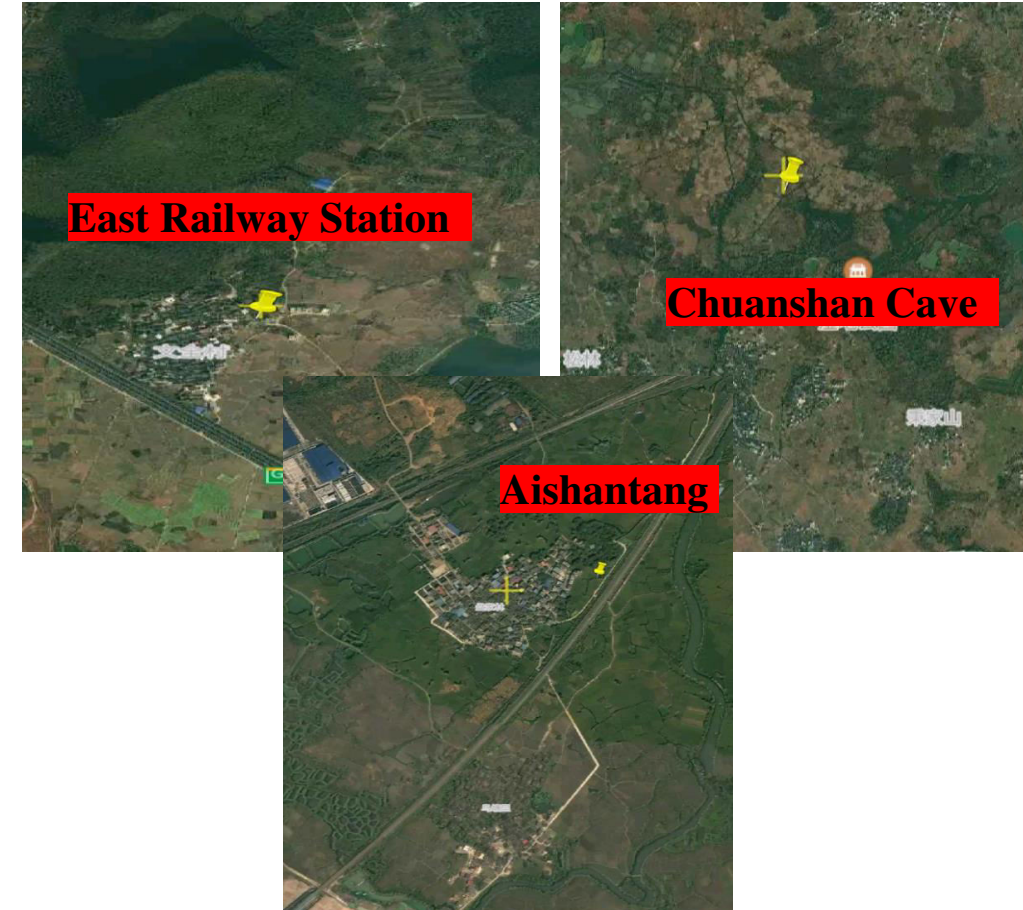
4.3 Spatial and temporal distribution of the main pollutants of groundwater quality



● Spatial and temporal distribution of Pb



Spatial distribution:



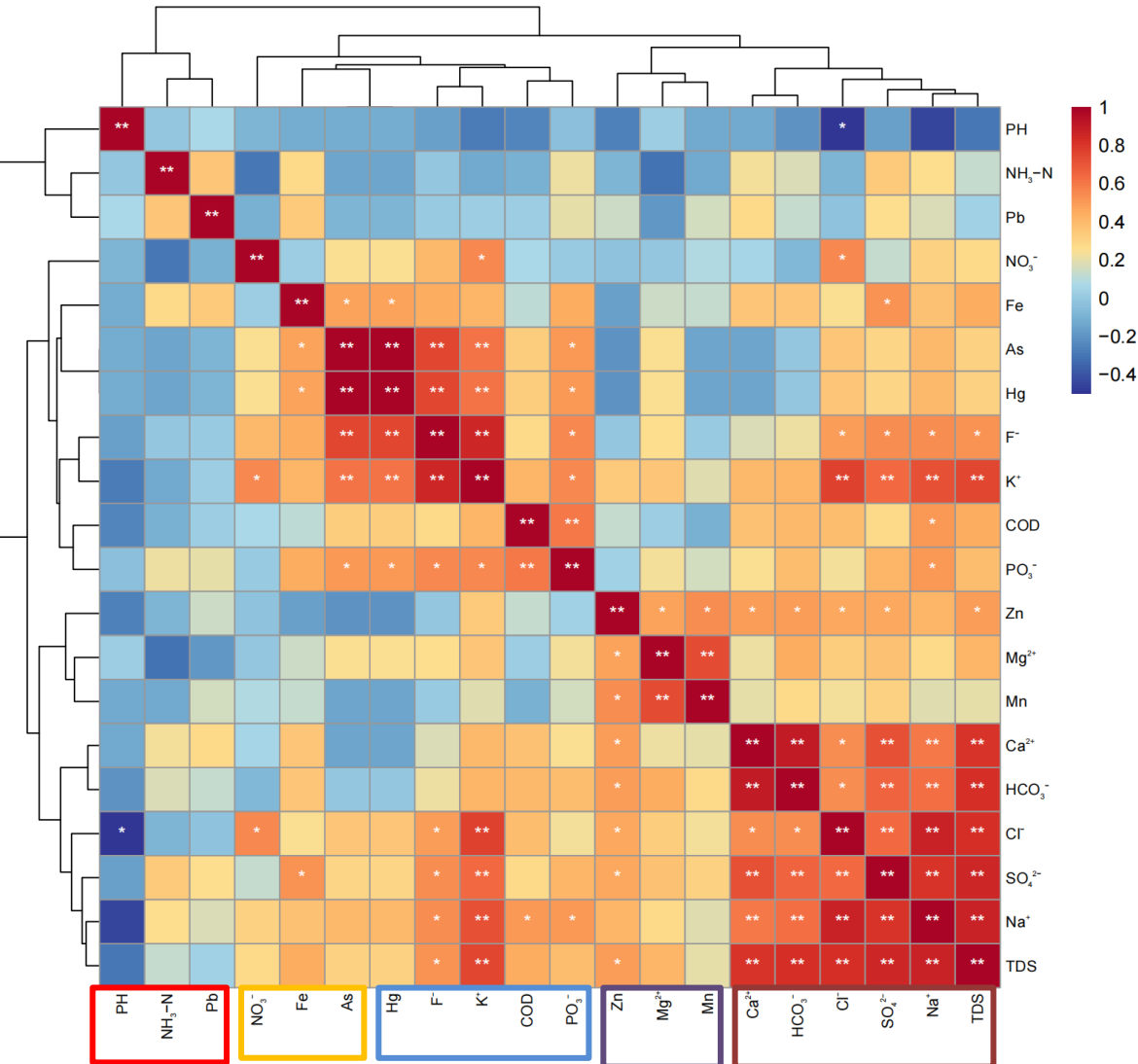
The Pb element is mainly distributed in the population gathering area.

4.3 Spatial and temporal distribution of the main pollutants of groundwater quality



2017

Correlation Heatmap



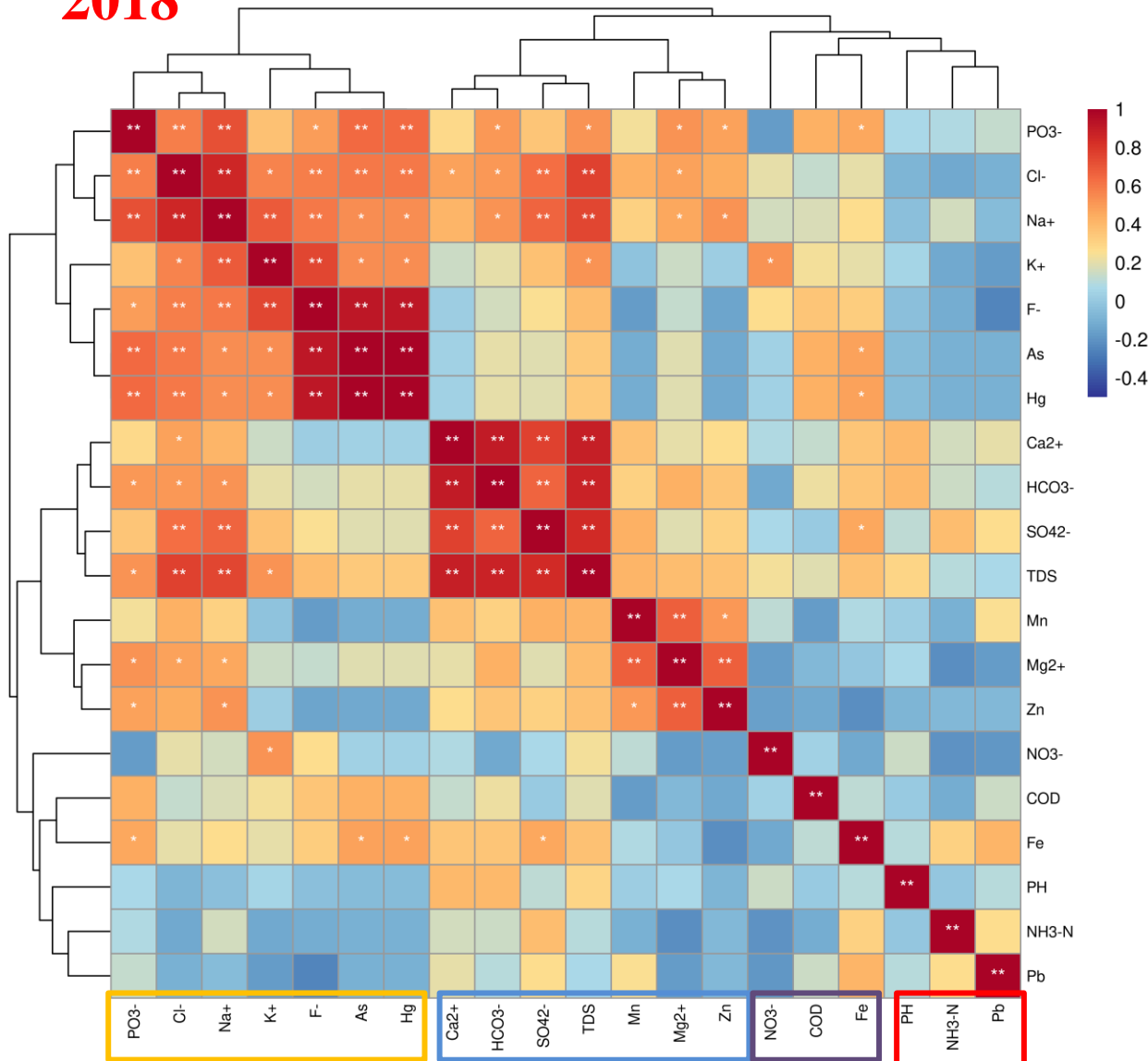
- Pb** and $\text{NH}_3\text{-N}$ re located in traffic areas such as railway stations, and studies have shown that automobile exhaust contains Pb, **the source of Pb may be related to dry and wet deposition of automobile exhaust emissions** (Sun, 2014).
- NO_3^- , Hg, Fe, As, K^+ , and F^-** in groundwater are mainly distributed in villages with intensive agricultural activities, and their higher concentrations, **NO_3^- and Hg may originate from agricultural activities** (Zhang, 2015).
- Sampling sites with higher Zn, Mg^{2+} , **Mn** are mostly located near Ximen Rice Noodle Industrial Zone, **Mn is mainly derived from industrial production wastewater** (Zhang et al., 2015).

4.3 Spatial and temporal distribution of the main pollutants of groundwater quality



Correlation Heatmap

2018



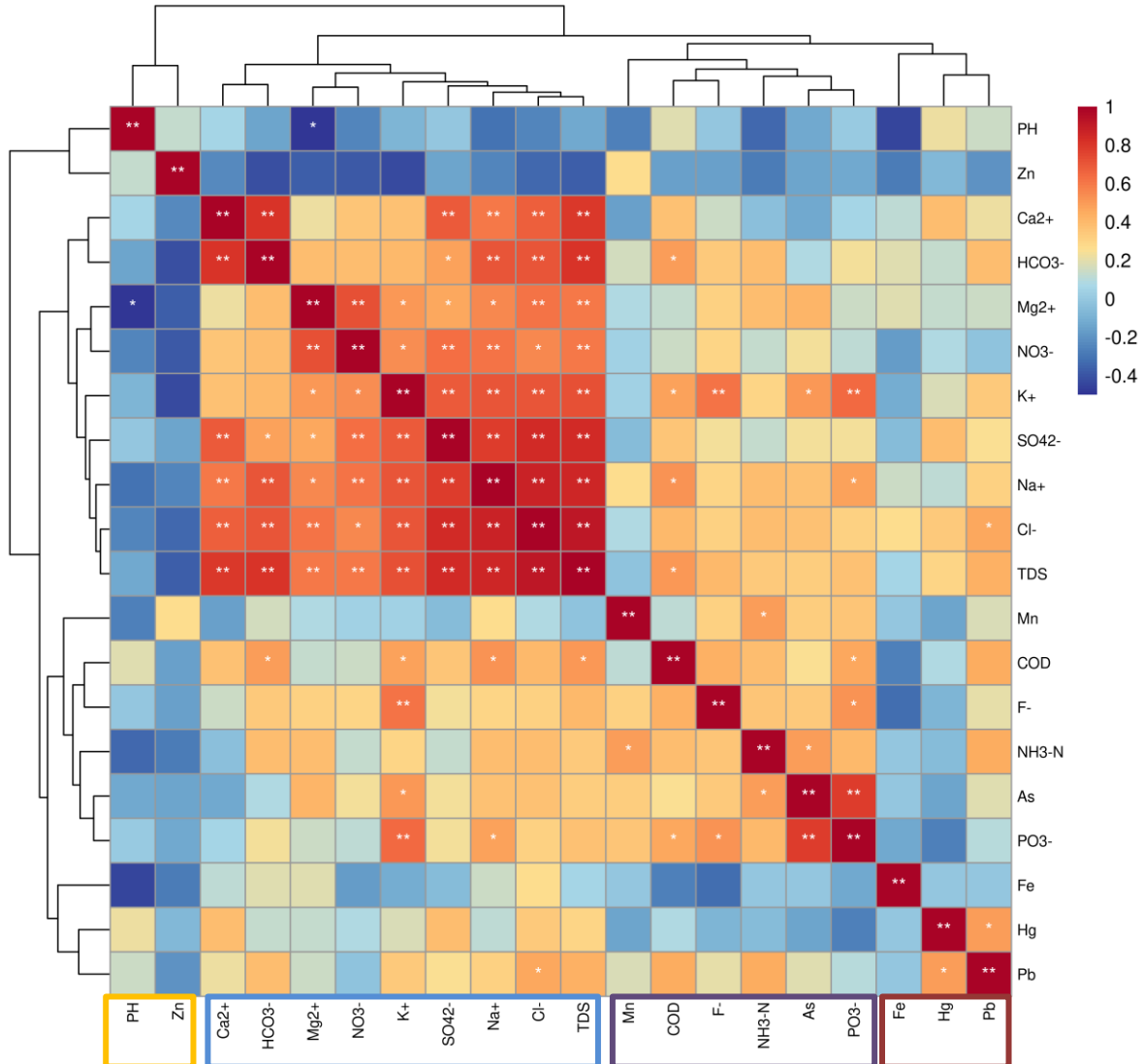
- The correlation between pH, NH₃-N, **Pb** is strong, Pb is a signature element of traffic activities (Cai Limei et al., 2004), mainly from car exhaust, etc., by NH₃-N, Pb is mainly distributed in the areas of high urban traffic, **which may be mainly related to car exhaust and municipal domestic waste.**
- The high correlation between **NO₃⁻**, **Hg** and K⁺ can be seen in the correlation heat map, then it may be related to the application of potash fertilisers (Zhang et al., 2023), **thus NO₃⁻ and Hg is mainly of agricultural origin.**
- Groundwater Zn and **Mn** contents are mainly controlled by natural factors, **Mn may be of geological origin (Liao et al., 2004).**

4.3 Spatial and temporal distribution of the main pollutants of groundwater quality



2019

Correlation Heatmap



- Compound fertiliser (KNO_3) is a common source of K^+ and NO_3^- ; suggesting that K^+ , Cl^- and KNO_3 are most likely derived from the application of fertilisers from **agricultural activities (Meng, 2020)**.
- The high correlation between **Pb**, **Hg**, Fe and mainly present in villages, could then be related to the landfill of domestic waste such as lead batteries and the application of lead-containing fertilisers (Wang et al., 2022; Zhang et al., 2018), and thus **Pb and Hg could originate from both domestic and agricultural activities**.
- **Mn**, $\text{NH}_3\text{-N}$, As, PO_3^- have the highest concentrations near industry, and industrial wastewater may contain Mn and As (Mo, 2010), **Mn mainly originate from industrial**.

5. Summary



Water quality assessment

- The temporal order of pollution is from greatest to least: **2017>2018>2019**, with cleaner water quality in 2019.
- Spatially the **degree of pollution** in the **West Zone** is worse than the **East Zone**, this is mainly related to the implementation of the **Environmental protection policy** and the **natural geographical advantages** of the Eastern District.

5. Summary



Identification of major pollutants

By comparing the single factor pollution indices of strongly polluted sampling sites in 2017, 2018 and 2019, the more polluted factors were screened as:

NO_3^- , Mn, Hg, Pb.

Where **NO_3^-** is the common pollution factor in 2017, 2018 and 2019;

Mn, Hg, Pb are more prominent pollution factors in 2018 and 2019.

5. Summary



Source analysis

Combined with the results of the source analysis of each factor in 2017-2019, there are diverse sources of each factor in the water body.

- NO_3^- and Hg is mainly from agricultural sources.
- Pb is mainly from vehicle exhaust, domestic waste and agricultural sources.

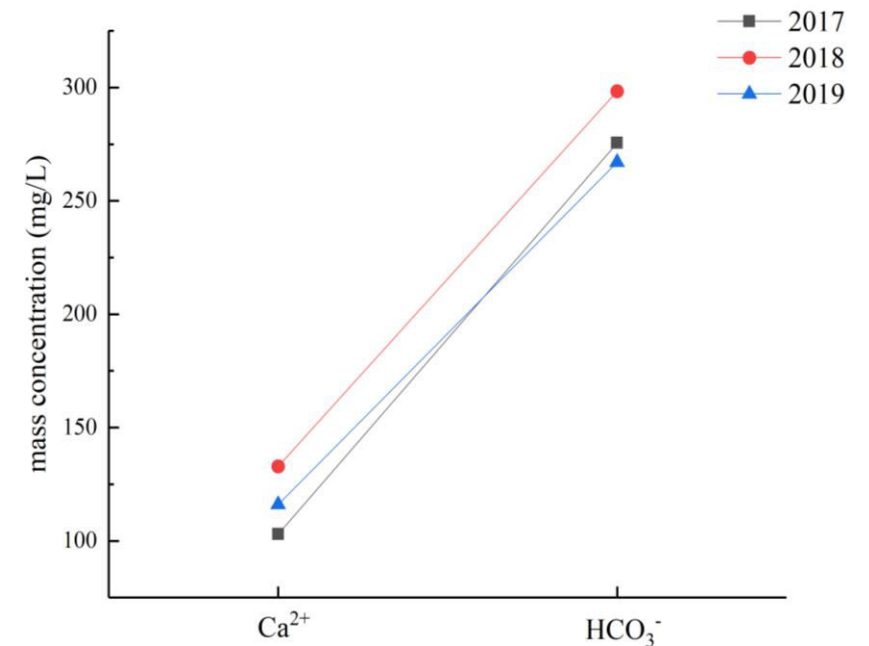
5. Summary



Source analysis

- Sources of Mn include geological and anthropogenic sources (industrial wastewater).
- 2018 : geological source
- 2017 and 2019 : anthropogenic sources

The reason for this discrepancy may be due to **enhanced weathering** of Mn-bearing rocks due to **higher rainfall** during the 2018 and the dilution effect on industrial and agricultural wastewater making the geological source of Mn dominant.



Stronger water-rock action in 2018

Thanks!

